JMEPEG (2021) 30:7909–7916
https://doi.org/10.1007/s11665-021-05977-w

1059-9495/$19.00

Effects of Non-isothermal Aging on Microstructure and Mechanical Properties of WE43 Alloy

Nazim Babacan, Emre Yurtkuran, Arif Balci, Magdalena Bieda-Niemiec, and Anna Jarzębska

Submitted: 26 January 2021 / Revised: 11 May 2021 / Accepted: 31 May 2021 / Published online: 1 July 2021

In the present work, the effect of non-isothermal aging (NIA) on the microstructural and mechanical properties of WE43 alloy was investigated by microhardness measurements, transmission electron microscopy observations and tensile tests. The effects of initial and secondary aging temperature and the heating/cooling rate of the NIA processes on the properties were systematically examined. While β″ precipitates formed during the continuous heating from 150 to 250 °C, secondary precipitation was observed in the continuously cooled samples from 250 to 150 °C. Similar mechanical properties compared to the peak-aged T6 sample (at 250 °C for 16 h) were obtained by NIA processes. However, continuous cooling, which leads to high mechanical properties after about 6 h of aging, was more efficient in time. NIA processes performed for the first time on Mg-Y-Nd-based alloys showed that high mechanical properties can be obtained in shorter period by tuning the properties of the precipitates.

Keywords magnesium alloy, mechanical property, non-isothermal aging, precipitates

1. Introduction

Magnesium alloys are used in many engineering applications where having a low weight is influential. Many components in aerospace and automotive industry are produced from magnesium alloys due to their low weight and high specific strength (Ref 1-3). Mg-rare earth (Mg–RE) alloys have recently attracted attentions as they have good mechanical properties with the combination of solid solution and precipitation hardening. Among these alloys, WE43 alloy stands out due to their good tensile properties, creep and corrosion resistance both at ambient and high temperatures (Ref 4-6). The strength of this alloy is mainly increased by precipitation hardening and the increase in the usage of this alloy depends on the development of mechanical properties such as strength and ductility (Ref 7).

The sequence of precipitation is observed as α-$(Mg)_{SSS}$-β'' (DO_{19})-β′ (cbco)-β_1 (fcc)-β_e (fcc) during the isothermal aging of a WE43 alloy (Ref 8-10). While β'' and β_1 phases are in the form of plate-like structures, β' phase can be in globular or plate shape. (Ref 9, 11-13). The type, morphology, size, volume ratio, and distribution of the precipitates are significant parameters that dictate the mechanical properties. Aging studies showed that the presence of β'' and β' precipitates in optimal proportions with a good distribution contribute greatly to the mechanical properties (Ref 9, 14, 15). Hardness and strength of WE43 alloy are increased industrially by heat treatment for 16 h at 250 °C, referred as T6. In addition, some studies have been carried out by performing different aging procedures in the literature.

Riontino et al. (Ref 14) studied microstructural changes after aging at 150, 210, 250 and 280 °C with different durations by performing DSC (differential scanning calorimetry) tests. DSC scans proved the formation of β'' precipitation at 150 °C, β'' and β' precipitates at 210 °C, β' and β_1 precipitates at 250 °C, β_1 and β_e 280 °C. Likewise, Mengucci et al. (Ref 8) confirmed those results using transmission electron microscopy (TEM) analysis in their study. The previous studies showed that peak-hardness value decreases with increasing the aging temperature from 175 to 250 °C (Ref 6, 9, 16, 17). Unlike the formation of large β_1 precipitates at 250 °C, the good combination of the small plate-shaped β'' and β' precipitates with a high density at lower temperatures create this difference. However, much longer aging durations are necessary to achieve the peak-hardness value at lower temperatures which is an important disadvantage for industrial applications.

Some researchers implemented different aging techniques to further increase the mechanical properties of WE43 alloy. Riontino et al. (Ref 15) adopted a two-step aging on WE 43 alloy and observed a further increment in the microhardness values. They obtained this improvement via the initial aging at 210 °C for 8 h and further aging at 150 °C. Secondary precipitations of β'' observed with the aging at 150 °C lead to an increase in microhardness by about 10%. However, they did not investigate the effect of this novel heat treatment on the mechanical properties. Kang et al. (Ref 9) also used two different techniques; the first one was 480 h of aging at 175 °C

Nazim Babacan, Department of Mechanical Engineering, Gazi University, Eti Mah. Yükseliş Sok. No: 5, 06570 Ankara, Turkey; Institute for Complex Materials, Leibniz IFW Dresden, Helmholtzstr. 20, 01069 Dresden, Germany; and Department of Mechanical Engineering, Sivas University of Science and Technology, Yenişehir Mah. Kardeşler Cad. No:7/1, 58140 Sivas, Turkey; **Emre Yurtkuran**, Department of Mechanical Engineering, Sivas University of Science and Technology, Yenişehir Mah. Kardeşler Cad. No:7/1, 58140 Sivas, Turkey; **Arif Balci**, Department of Mechanical Engineering, Kafkas University, Merkez Kampüsü, 36100 Kars, Turkey; **Magdalena Bieda-Niemiec** and **Anna Jarzębska**, Institute of Metallurgy and Materials Science of Polish Academy of Sciences, 25 Reymonta St, 30-059 Krakow, Poland. Contact e-„mail: nazimbabacan@sivas.edu.tr.

+ different periods of aging at 250 °C and the second one was aging at 250 °C for 8 h + 168, 360 and 600 h of aging at 175 °C. In the first aging process, although β'' precipitations were expected to be transform directly to β' phase, they directly dissolved. Therefore, an increase in the mechanical properties sourced from the coexistence of β'' and β' phases could not be achieved. On the other hand, although the yield strength was improved due to secondary β'' and β' precipitations, the elongation at fracture decreased to 1.7% in 168 h and to 0.5% in 600 h from 4% in the second two-step aging technique.

While above-mentioned aging techniques were performed in the last decades, there is still need for an effective aging procedure to obtain high mechanical properties at shorter times which gives an opportunity to reduce the operational costs for Mg–RE alloys. A novel and efficient continuous heating or cooling heat treatment cycle can be designed to a produce Mg alloys with superior mechanical properties. This heat treatment process creates a condition of enhanced diffusion of solutes at high aging temperature and provides a condition for triggering precipitates at lower temperature. Properties of precipitates such as size and morphology can be tuned with/without secondary precipitate formation and thus, optimal parameters which enhance the mechanical properties can be obtained due to this non-isothermal aging (NIA) processes. Most studies on NIA have focused on Al-Zn-Mg-Cu alloys (Ref 18-21) and there is no decisive study of the effect of NIA on the mechanical response in Mg-RE alloys.

The present study concerns with the effect of NIA on WE43 alloy in terms of change in microstructural and mechanical properties. Transmission electron microscope was used to characterize precipitates after conventional isothermal and different type of NIA steps and the microstructural observations were correlated with the mechanical test results. Specifically, it was planned to investigate the effect of different NIA procedures on the microhardness and obtain comparable mechanical properties with T6 aging treatment in less time.

2. Experimental Procedures

The as-received alloy (Mg-4Y-2.5Nd-1.2Gd-0.5Zr wt%) was obtained in the form of extruded billet. This alloy was solution treated at a temperature of 525 °C for 8 h and then quenched into water. While some part of the solutionized samples were aged at 250 °C for various durations, remaining parts were non-isothermally aged by using the procedure shown in Table 1. After each aging treatment, the samples were quenched in water. For simplification, the specimens were named as follows: (1) initial aging temperature-(2) secondary temperature/(3) heating or cooling rate. For example, the sample was initially aged at 150 °C for 2 h and then heated to 250 °C with 10 °C/h was named as 150-250/10.

Microstructural characterization was performed using transmission electron microscope. Samples were prepared on a twin jet electro polisher using a solution consisting of 750 ml AR grade methanol, 150 ml butoxyethanol, 16.74 g magnesium perchlorate and 7.95 g lithium chloride. Analysis was executed by means of FEI-Tecnai G2 F20 equipped with energy-dispersive X-ray spectroscopy (EDS) and High Angle Annular Dark Field (HAADF). Electron diffraction registered in transmission electron microscope was analyzed using CSpot software (CrystOrient, Zabierzów, Poland). Precipitation length analysis was performed using ImageJ® software.

Vickers microhardness (HV) testing was performed by applying 500 g load for 10 s and average of ten measurements was taken from each sample. Tensile tests were performed at room temperature with a strain rate of $5x10^{-4}$ s^{-1} using an Instron 5869 device and the strain was measured directly on the specimens with a Fiedler laser-extensometer. Dog-bone-shaped tension samples with a gage length of 16.6 mm and with a width of 2.25 mm were cut using a wire electrical discharge machining and three specimens were used for each condition.

3. Results and Discussion

3.1 Microhardness

Microhardness values of aged samples for different durations at 250 °C are shown in Fig. 1. The trend of change of hardness values according to the aging time is comparable with the literature (Ref 6, 8, 9, 22). The highest hardness value (97.8 HV) was obtained with 16 h of aging (T6).

In this study, NIA treatments are divided into 2 parts:

1. In order to tune the β'' or/and enable the transformation of β'' into different volume ratios of β' and β_1 precipitates; the samples were initially aged at 150 °C for 2 h and then they were heated to three different temperatures, 210, 230 and 250 °C, respectively, with different heating rates.
2. The samples were initially aged for 2 h at 250 °C and

Table 1 NIA processes applied to as-quenched samples (heating rate to initial temperature: 10 °C/min, waiting period in the initial temperature: 2 h)

Initial temperature, °C	Secondary temperature, °C	Heating or cooling rate, °C/h
150	210	10
		20
		30
	230	10
		20
		30
	250	10
		20
		30
250	150	10
		20
		30

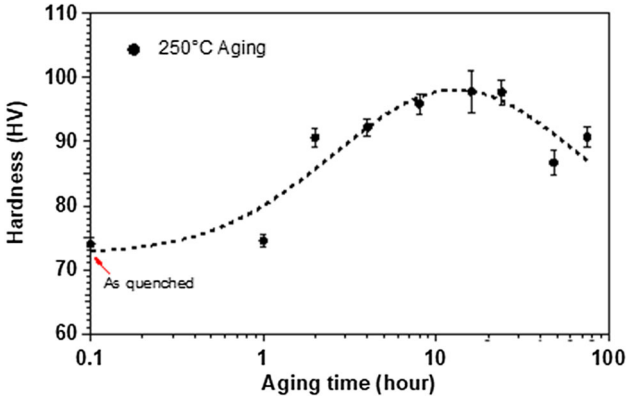

Fig. 1 Microhardness chage of WE43 alloy as a function of aging time at the temperature of 250 °C

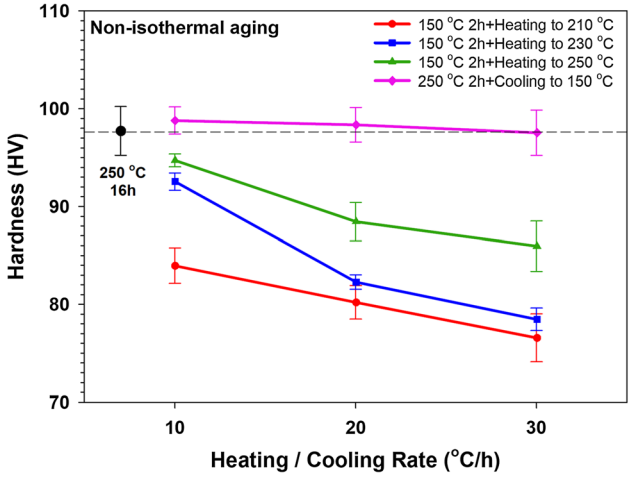

Fig. 2 Microhardness values obtained as a result of NIA treatments obtained with different heating/cooling rates

then cooled to 150 °C using different cooling rates, for the formation of secondary precipitates.

Figure 2 shows the microhardness values obtained after NIA treatments. The hardness value of T6 sample was also added for comparison. The microhardness values of the samples heat treated at 250 °C are higher than 210 and 230 °C, among the initially 150 °C aged samples. Since heating to 210 and 230 °C with defined heating rates did not give the time required for precipitates to reach sufficient density, the hardness levels were not too high. Moreover, a pronounced decrease in hardness occurs as the heating rate increases. This is again in accordance with the time required to achieve the sufficient precipitate density. The increase in the heating rate caused a decrease in the aging time, which resulted a decrease in the hardness value.

The hardness values of the samples, which were initially aged at 250 °C for 2 h and then cooled to 150 °C, are comparable with that of the T6 sample. Furthermore, unlike the first part, no significant change in hardness values is observed as the cooling rates changed.

3.2 Microstructural Analysis

Four samples which have high hardness values (T6; 150-250/10; 250-150/30; 250-150/10) were examined by transmission electron microscope. These samples were selected to compare the microstructural differences occuring with isothermal and NIA heat treatments with continuous heating and cooling.

Figure 3 shows the various sizes of globular precipitates (β') located in the grain boundary of T6 sample. Moreover, bimodal distribution of the β type precipitates is observed among the microstructure. Smaller ones (Fig. 3c) are associated with the β' phase considering the extra spots appear at 1/4 $[01\bar{1}0]_{Mg}$, 1/2 $[01\bar{1}0]_{Mg}$ and 3/4 $[01\bar{1}0]_{Mg}$ on the diffraction pattern along $[11\bar{2}0]_{Mg}$ (as shown in Fig. 3b) (Ref 9, 10, 23, 24). Larger precipitates (Fig. 3e) are β_1 phase with fcc crystal structure as seen in the peak-aging studies of Mg alloys at 250 °C (Ref 8, 9, 11, 25, 26). Both type of precipitates is elongated along □0001□$_{Mg}$ direction (Ref 22, 26). Length distribution histograms located in Fig. 3(d, f) reveal that while average length of the β' is about 60 nm, average length of β_1 precipitates is around 280 nm.

Figure 4 shows the TEM images of the 150–250/10 sample. Uniformly fine dispersed β'' precipitates inside the grains and large overlapped precipitates along the grain boundary which are composed from Mg, Y and Nd elements are observed in the BF and HAADF images (Fig. 4a, b) (Ref 13, 27). Moreover, a few cuboid-shaped particles are detected near the grain boundaries. The average length of the plate-like precipitates oriented in <0001> direction is about 30 nm. Barucca et al. (Ref 28) observed small β'' plate-like precipitates with size ranging from 0.5 to 2 nm for WE43 alloy submitted to 150 °C aging for 12 days. Thus, NIA with continuous heating starting from 150 °C triggered the formation of larger β'' precipitates in much shorter times. This treatment can be an opportunity for tuning the size of plate-like β'' precipitates effectively and lead to achieve optimal precipitate length and distribution in much shorter times. On the other hand, TEM investigations showed that β'' did not transform into neither β' nor β_1 precipitates during the continous heating.

Microhardness results obtained with the continuous heating (Fig. 2) can be better evaluated based on this microstructural investigation. Heating to 250 °C with 10 °C/h created the condition for maximum diffusion among all the initially aged samples at 150 °C. Precipitate length increases as the diffusion rate increases, which leads to increase in microhardness value until peak-aging condition is achieved. Therefore, increasing the secondary temperature, or decreasing the heating rate increases the hardness.

Figure 5(a, b) illustrates TEM BF images of the 250-150/30 sample and the corresponding histogram of the length of the precipitates, respectively. The average length of the precipitates was calculated to be approximately 60 nm in <0001> direction. Moreover, globular-shaped precipitates are also observed in Fig. 5 (c). On the diffraction pattern along $[0001]_{Mg}$ axis zone (Fig. 5d), extra spots that belong to the β' phase are visible. The maximum intensity in 1/2 $[01\bar{1}0]_{Mg}$ also proves the existence of β'' precipitates in the sample (Ref 9, 28). Platelet precipitates are in contact with globular phases as seen in Fig. 5(e) which are the characteristics of β_1 precipitates (Ref 6, 8, 11, 29). Kang et al. (Ref 6) also observed β_1 precipitates after holding of WE43 sample at 250 °C for 2 h with the small β' precipitates in their study.

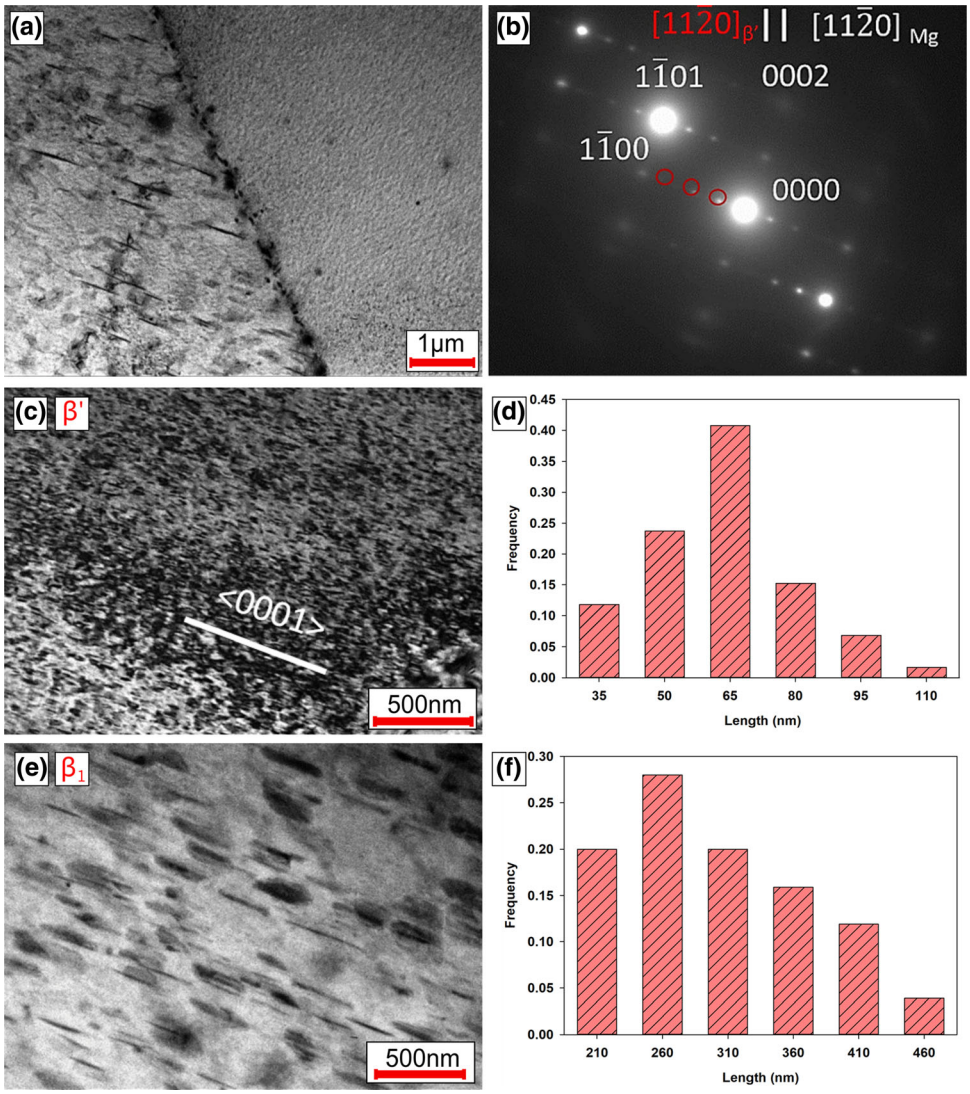

Fig. 3 TEM BF images showing (a) two different grains with a grain boundary, (b) SAED pattern along $[11\bar{2}0]$Mg axis for T6 sample, (c) small precipitates (β') , (d) corresponding length distrubition histogram for β_1 precipitates (e) large precipitates (β_1) and (f) corresponding length distrubition histogram for β' precipitates

TEM investigations show the existence of β", β' and β_1 precipitates in the 250-150/30 sample. Hence, a part of the solute atoms still retains in the microstructure such that cooling to lower temperature after 250 °C/ 2 h aging provides sufficient driving force for the formation of secondary precipitates. Thus, high microhardness values in the NIA condition with continuous cooling (Fig. 2) could be attributed to positive effect of the secondary precipitates.

BF image of 250-150/30 sample presented in Fig. 6(a) shows the precipitates in <0001> direction. Average length of these precipitates was calculated as approximately 85 mm from the corresponding histogram in Fig. 6(b). The precipitate size is about 25 nm higher compared to that of 250-150/10. All the average lengths with the standard deviations calculated from the measured length of precipitates are compared in Table 2 Although it is not clear whether the precipitates shown in Fig. 6 (a) are β" or β', a slight increase in the microhardness observed with the decrease in cooling rate could be attributed to the larger secondary (β") or β' precipitates that nucleated with more time.

3.3 Tensile Properties

Four differently aged pieces with high hardness values were subjected to tensile tests in order to investigate the role of NIA on tensile properties. The representative engineering stress-strain curves of four conditions are represented in Fig. 7.

Table 3 shows the yield strengths, ultimate tensile strengths and tensile elongations with their standard deviations calculated from these tests. While the highest strength values are observed after the 250-150/10 aging treamet, no significant difference in all the mechanical properties between the samples was found.

Precipitate type and morphology are influential factors for mechanical parameters. It is known that plate-shaped precipitates are considered to most effective shape for the strengthening of Mg-Y-Nd based alloys since they would capably prevent basal slip (Ref 30-32). TEM BF images in this study prove that the main precipitate morphology is plate-shaped in all aging conditions. TEM investigations revealed that 150-250/10 sample has only β" precipitates with approximately 30 nm average length. Kang et al. (Ref 9) observed about 10-20 nm

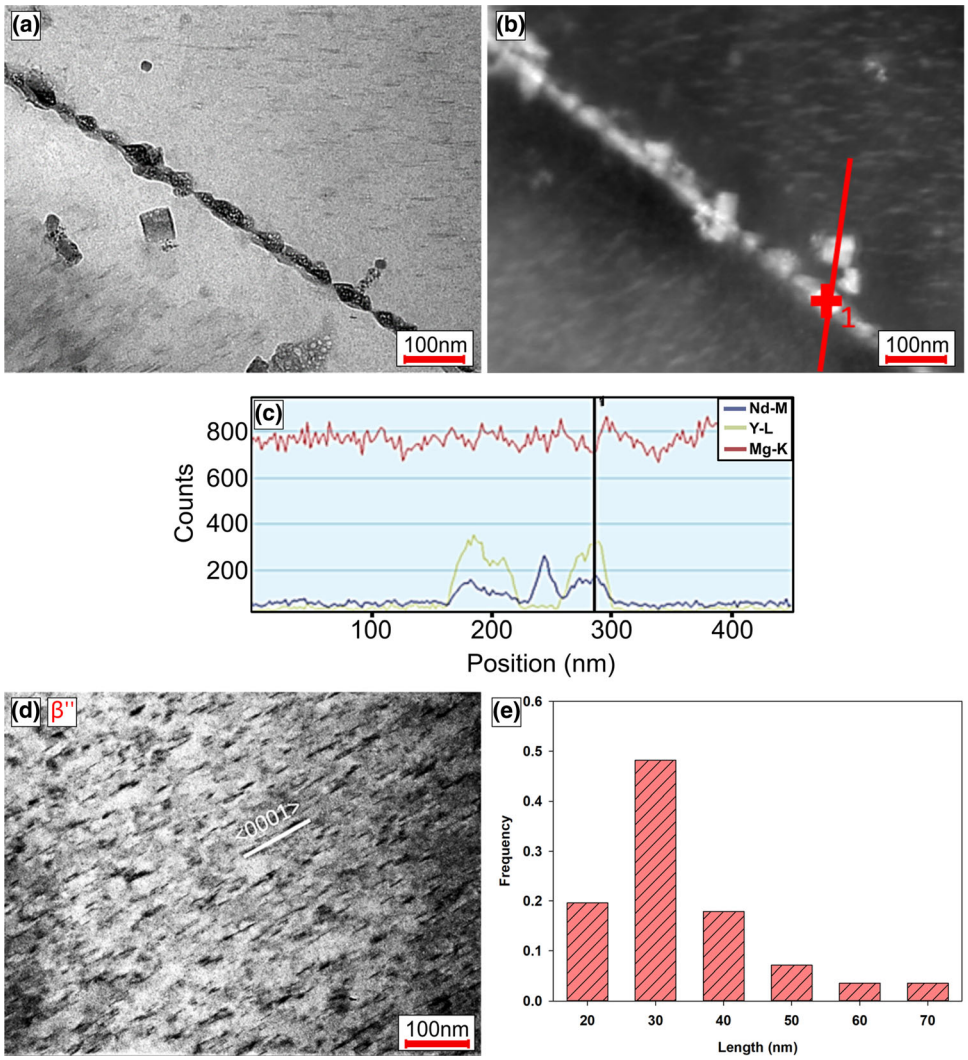

Fig. 4 (a) TEM BF image and (b) corresponding HAADF image with (c) EDS line scan across the grain, (d) BF image and (e) corresponding precipitation length distrubition histogram of 150-250/10 sample

plate-shaped precipitates which are mostly β'' type precipitates after the peak-aging condition at 175 °C for 480 h. The microhardness value of this sample is higher than that of the peak-aged sample at 250 °C. Therefore, high mechanical properties of 150-250/10 sample could be attributed to the significant distrubition of the plate-shaped β'' precipitates that have average length values close to the optimum. In addition, mechanical properties similar to the peak-aged sample at 250 °C were achieved in only around 12 h as an advantage by fast tuning the size of the precipitates with NIA with continuous heating.

The mechanical test results of 250-150/30 sample are also very close to the those of the reference T6 sample. As a result of the TEM analysis made on 250-150/30 sample, it was found that β'' precipitates exist in addition to β' and β_1 precipitates due to the occurence of secondary precipitation. It is believed that the combination of these three type precipitates mostly having plate shape lead to obtain good mechanical properties in such a short time (less than 6 h).

Tensile tests on the 250-150/10 samples were perfomed to evaluate the influence of cooling rate on the mechanical properties, for the continuous cooling aging treatment. Decrease in cooling rate from 30 to 10 °C/h caused no other effect other than a slight increase in the yield strength. Since the cooling rate is lower, larger secondary precipitate or β' formation is more likely to occur in this sample as seen in the length calculations increasing from 60 to 85 nm. This small enhancement is also seen in the microhardness values as the cooling rate was decreased. Although the cooling rate parameter appears to have an effect on the mechanical properties, this effect is relatively minor compared to the heating rate, as seen in the continuously heated samples.

Considering that 250-150/10 and 250-150/30 samples have similar microstructures, three different types of microstructure showed similar mechanical behavior as a result of the tensile tests. Thus, it implies that the samples exposed to NIA heat treatment have a near-optimum precipitation size and distribution as in T6 peak-aging condition. While β'' precipitates with an average length of 30 nm in the 150-250/10 sample could provide this condition, the good combination of β'', β' and β_1 precipitates is thought to lead a high yield strength for 250-150/10 and 250-150/30 samples. Moreover, coherency of the precipitates with Mg matrix is an important aspect for evaluating the mechanical properties such as microhardness

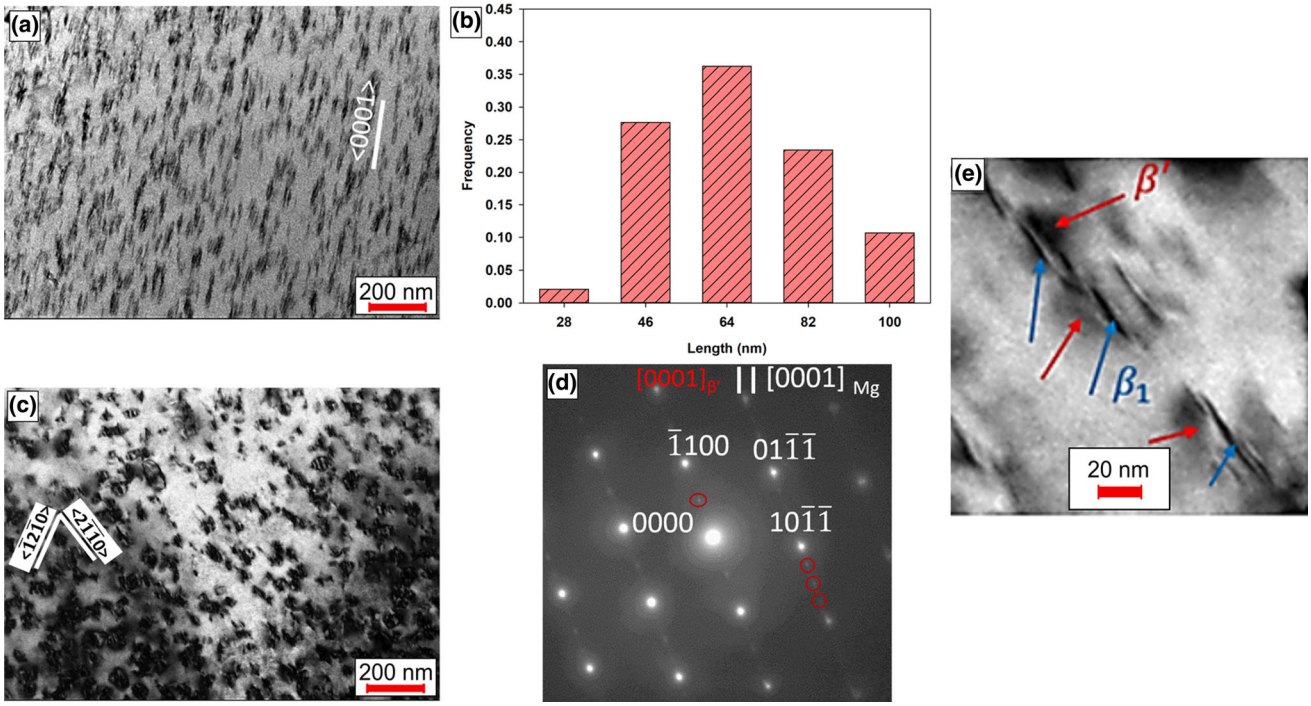

Fig. 5 (a) TEM BF image and (b) corresponding length distrubition histogram of precipitates (c) TEM BF image and (d) corresponding SAED pattern along $[0001]_{Mg}$ axis zone (e) magnified view of several precipitates 250-150/30 sample

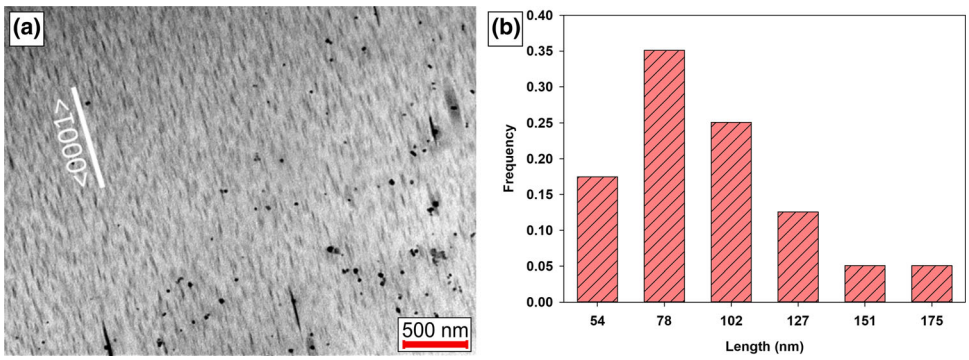

Fig. 6 (a) TEM BF image and (b) corresponding precipitation length distrubition histogram of 250-150/10 samples

Table 2 Average lengths of precipitates with the standart deviations

	T6				
	β_1	β'	150-250/10	250-150/30	250-150/10
Average length (nm)	278 ± 71	56 ± 16	28 ± 11	57 ± 17	84 ± 32

values. While β″ phase was found to be fully coherent with Mg matrix, β′ phase was found to be coherent/semicoherent in the literature (Ref 7, 9, 27, 28, 33). These precipitates are the dominant precipitate types in the mechanically tested NIA-aged alloys (150-250/10, 250-150/10, 250-150/30). Hence, stress fields around these phases lead to significant strength enhancement as they act as effective barriers for dislocation slip.

Moreover, contrary to large amount of drop in the elongation in the study of Kang et al. (Ref 9) after two-step aging (initially at 250 °C and then at 175 °C), similar elongation values were obtained for 250-150/10 and 250-150/30 samples with the isothermally aged sample. However, the reason beyond that is not clear yet. It is known that besides the precipitate type and morphology, many parameters like thickness, aspect ratio, density of the precipitates have an important role on the mechanical properties (Ref 22, 32). Therefore, a more comprehensive study is needed to be done in order to better evaluate the effect of different NIA procedures on the microstructural and mechanical properties. However, this study definitely shows the success of NIA on tuning the microstruc-

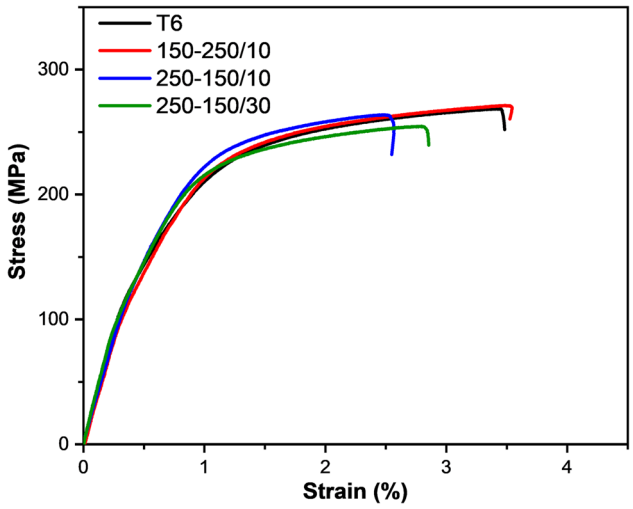

Fig. 7 The tensile stress-strain curves of the investigated alloys

Table 3 Tensile properties of isothermal and non-isothermally aged alloys

Condition	Yield strength (MPa)	Ultimate tensile strength (MPa)	Elongation (%)
T6	186 ± 15	268 ± 5	3.0 ± 0.4
150-250/10	181 ± 14	265 ± 10	3.3 ± 0.2
250-150/30	184 ± 6	266 ± 9	3.2 ± 0.4
250-150/10	192 ± 14	263 ± 5	3.1 ± 0.7

ture of WE43 magnesium alloy. More generally, this research has revealed that there are other opportunities to obtain high mechanical properties in a shorter period than the conventional single-step aging for Mg-Y-Nd-based alloys.

4. Conclusions

The main findings and conclusions were summarized as follows:

1. Examination of the WE43 samples, which were aged 150 °C for 2 h and then heated to 210, 230 and 250 °C with the rates of 10, 20 and 30 °C, showed that the microhardness values increases when the secondary heating temperature is increased and the heating rate is decreased. This is attributed to increase in the amount of β" and its positive effect on microhardness.
2. Comparable hardness values with isothermal aging were obtained in shorter times by using NIA. The highest hardness values were achieved in NIA samples that were aged at 250 °C for 2 h and then cooled to 150 °C. Decrease in the cooling rate caused a slight increase in the microhardness and yield strength. Difference in the amount and the size of secondary precipitates are believed to dictate this change.
3. 250-150/30 sample which was subjected to less than 6 h aging showed comparable mechanical properties with conventionally 16 h aged sample at 250 °C.
4. It has been observed that precipitate properties such as size and morphology can be changed, and new secondary precipitates can be formed with NIA processes. This situation shows that the microstructure of WE43 alloy can be easily tuned and the high mechanical properties can be achieved with the NIA processes performed in shorter times.

Acknowledgment

This research has been supported by Gazi University BAP through Project No. 06/2018-07. N. Babacan thanks Dr. Avinash Hariharan (IFW Dresden) for his help in critical reading of the manuscript.

Data Availability

The data supporting the findings of this study are available from the corresponding author on reasonable request.

Conflicts of interest

The author declared that there is no conflict of interest

References

1. I.J. Polmear, Magnesium Alloys and Applications, *Mater. Sci. Technol.*, 1994, **10**, p 1–16
2. H. Friedrich and S. Schumann, Research for a "New Age of Magnesium" in the Automotive Industry, *J. Mater. Process. Technol.*, 2001, **117**, p 276–281
3. T. Pollock, Weight Loss with Magnesium Alloys, *Science*, 2010, **328**, p 986–987
4. Y. Chen, Z. Xu, C. Smith and J. Sankar, Recent Advances on the Development of Magnesium Alloys for Biodegradable Implants, *Acta Biomater.*, 2014, **10**(11), p 4561–4573
5. P.J. Apps, H. Karimzadeh, J.F. King and G.W. Lorimer, Precipitation Reactions in Magnesium-Rare Earth Alloys Containing Yttrium, Gadolinium or Dysprosium, *Scr. Mater.*, 2003, **48**(8), p 1023–1028
6. Y.H. Kang, X.X. Wang, N. Zhang, H. Yan and R.S. Chen, Effect of Initial Temper on the Creep Behavior of Precipitation-Hardened WE43 Alloy, *Mater. Sci. Eng. A*, 2017, **689**, p 419–426
7. S.K. Panigrahi, W. Yuan, R.S. Mishra, R. Delorme, B. Davis, R.A. Howell and K. Cho, A Study on the Combined Effect of Forging and Aging in Mg–Y–RE Alloy, *Mater. Sci. Eng. A*, 2011, **530**, p 28–35
8. P. Mengucci, G. Barucca, G. Riontino, D. Lussana, M. Massazza, R. Ferragut and E.H. Aly, Structure Evolution of a WE43 Mg Alloy Submitted to Different Thermal Treatments, *Mater. Sci. Eng. A*, 2008, **479**(1–2), p 37–44
9. Y.H. Kang, H. Yan and R.S. Chen, Effects of Heat Treatment on the Precipitates and Mechanical Properties of Sand-Cast Mg–4Y–2.3 Nd–1Gd–0.6 Zr Magnesium Alloy, *Mater. Sci. Eng. A*, 2015, **645**, p 361–368
10. H. Zhang, J. Fan, L. Zhang, G. Wu, W. Liu, W. Cui and S. Feng, Effect of Heat Treatment on Microstructure, Mechanical Properties and Fracture Behaviors of Sand-Cast Mg-4Y-3Nd-1Gd-0.2 Zn-0.5 Zr Alloy, *Mater. Sci. Eng. A*, 2016, **677**, p 411–420
11. C. Antion, P. Donnadieu, F. Perrard, A. Deschamps, C. Tassin and A. Pisch, Hardening Precipitation in a Mg-4Y-3RE Alloy, *Acta Mater.*, 2003, **51**(18), p 5335–5348
12. H.S. Jiang, M.Y. Zheng, X.G. Qiao, K. Wu, Q.Y. Peng, S.H. Yang, Y. H. Yuan and J.H. Luo, Microstructure and Mechanical Properties of WE43 Magnesium Alloy Fabricated by Direct-Chill Casting, *Mater. Sci. Eng. A*, 2017, **684**, p 158–164

13. S. Kandalam, R.K. Sabat, N. Bibhanshu, G.S. Avadhani, S. Kumar and S. Suwas, Superplasticity in High Temperature Magnesium Alloy WE43, *Mater. Sci. Eng. A*, 2017, **687**, p 85–92
14. G. Riontino, D. Lussana and M. Massazza, A Calorimetric Study of Phase Evolution in a WE43 Mg Alloy, *J. Therm. Anal. Calorim.*, 2006, **83**(3), p 643–647
15. G. Riontino, M. Massazza, D. Lussana, P. Mengucci, G. Barucca and R. Ferragut, A Novel Thermal Treatment on a Mg-4.2Y-2.3Nd-0.6Zr (WE43) Alloy, *Mater. Sci. Eng. A*, 2008, **494**(1), p 445–448
16. H. Li, F. Lv, X. Liang, Y. Qi, Z. Zhu and K. Zhang, Effect of Heat Treatment on Microstructures and Mechanical Properties of a Cast Mg-Y-Nd-Zr Alloy, *Mater. Sci. Eng. A*, 2016, **667**, p 409–416
17. S. Kandalam, P. Agrawal, G.S. Avadhani, S. Kumar and S. Suwas, Precipitation Response of the Magnesium Alloy WE43 in Strained and Unstrained Conditions, *J. Alloys Compd.*, 2015, **623**, p 317–323
18. Y. Liu, D. Jiang, B. Li, W. Yang and J. Hu, Effect of Cooling Aging on Microstructure and Mechanical Properties of an Al-Zn-Mg-Cu Alloy, *Mater. Des.*, 2014, **57**(2), p 79–86
19. D. Jiang, Y. Liu, S. Liang and W. Xie, The Effects of Non-Isothermal Aging on the Strength and Corrosion Behavior of Al-Zn-Mg-Cu Alloy, *J. Alloys Compd.*, 2016, **681**, p 57–65
20. Y. Liu, S. Liang and D. Jiang, Influence of Repetitious Non-Isothermal Aging on Microstructure and Strength of Al-Zn-Mg-Cu Alloy, *J. Alloys Compd.*, 2016, **689**, p 632–640
21. J.T. Jiang, Q.J. Tang, L. Yang, K. Zhang, S.J. Yuan and L. Zhen, Non-isothermal Ageing of an Al-8Zn-2Mg-2Cu Alloy for Enhanced Properties, *J. Mater. Process. Tech.*, 2016, **227**, p 110–116
22 Y.H. Kang, D. Wu, R.S. Chen and E.H. Han, Microstructures and Mechanical Properties of the Age Hardened Mg-4.2Y-2.5Nd-1Gd-0.6Zr (WE43) Microalloyed with Zn, *J. Mag. Alloys*, 2014, **2**(2), p 109–115
23. R. Zheng, T. Bhattacharjee, S. Gao, W. Gong, A. Shibata, T. Sasaki, K. Hono and N. Tsuji, Change of Deformation Mechanisms Leading to High Strength and Large Ductility in Mg-Zn-Zr-Ca Alloy with Fully Recrystallized Ultrafine Grained Microstructures, *Sci. Rep.*, 2019, **9**(1), p 1–2
24. J.F. Nie and B.C. Muddle, Characterisation of Strengthening Precipitate Phases in a Mg–Y–Nd Alloy, *Acta Mater.*, 2000, **48**, p 1691–1703
25. X.Z. Han, W.C. Xu, L. Yuan and D.B. Shan, Microstructure Evolution and Mechanical Properties of High Performance Mg-10Gd-2Y-0·5Zn-0·3Zr Alloy During Heat Treatments, *Mater. Sci. Technol. (United Kingdom)*, 2013, **29**(9), p 1065–1073
26. Q.Y. Sun, L.P. Wang and D.R. Liu, Effects of Pre-Stretching on Microstructure and Properties of WE43A-Alloy after Aging Treatment, *Mater. Sci. Technol. (United Kingdom)*, 2019, **35**(12), p 1448–1456
27. M. Bamberger, G. Atiya, S. Khawaled and A. Katsman, Comparison Study of Microstructure and Phase Evolution in Mg-Nd- and Mg-Gd-Based Alloys, *Metall. Mater. Trans. A*, 2014, **45**(8), p 3241–3253
28. G. Barucca, R. Ferragut, F. Fiori, D. Lussana, P. Mengucci, F. Moia and G. Riontino, Formation and Evolution of the Hardening Precipitates in a Mg-Y-Nd Alloy, *Acta Mater.*, 2011, **59**(10), p 4151–4158
29. Y.H. Kang, Z.H. Huang, S.C. Wang, H. Yan, R.S. Chen and J.C. Huang, Effect of Pre-Deformation on Microstructure and Mechanical Properties of WE43 Magnesium Alloy II:Aging at 250 and 300 ° C, *J. Magnes. Alloy.*, 2020, **8**(1), p 103–110
30. X. Zhang, C. Tang, Y. Deng and L. Yang, Effects of Thermal Treatment on Precipitate Shape and Mechanical Properties of Mg-8Gd-4Y-Nd-Zr Alloy, *Mater. Des.*, 2011, **32**(10), p 4994–4998
31. S.R. Agnew, R.P. Mulay, F.J.P. Iii, C.A. Calhoun and J.J. Bhattacharyya, In Situ Neutron Diffraction and Polycrystal Plasticity Modeling of a Mg–Y–Nd–Zr Alloy:Effects of Precipitation on Individual Deformation Mechanisms, *Acta Mater.*, 2013, **61**(10), p 3769–3780
32. L. Xu, C. Liu, Y. Wan, X. Wang and H. Xiao, Effects of Heat Treatments on Microstructures and Mechanical Properties of Mg–4Y–2.5Nd–0.7Zr Alloy, *Mater. Sci. Eng. A*, 2012, **558**, p 1–6
33. F. Penghuai, P. Liming, J. Haiyan, Z. Zhenyan and Z. Chunquan, Fracture Behavior and Mechanical Properties of Mg-4Y-2Nd-1Gd-0.4Zr (Wt.%) Alloy at Room Temperature, *Mater. Sci. Eng. A*, 2008, **486**(1–2), p 572–579